

Anchoring Energies of Liquid Crystals Measured on Surfaces Presenting Oligopeptides

Brian H. Clare, Orlando Guzmán, Juan de Pablo, and Nicholas L. Abbott*

Department of Chemical and Biological Engineering, University of Wisconsin-Madison,
1415 Engineering Drive, Madison, Wisconsin 53706

Received February 16, 2006. In Final Form: May 25, 2006

We report a methodology that permits quantitation of the azimuthal anchoring energy of the nematic liquid crystal 4-cyano-4'-pentyl-biphenyl on surfaces patterned with oligopeptides. The oligopeptide (IYGEFKKKC), an optimized substrate for the Src protein kinase, was covalently immobilized via the terminal cysteine to monolayers of amine-terminated tetra(ethylene glycol) formed on gold films. The measurements of anchoring energies, which were based on a torque-balance method, revealed a systematic decrease in anchoring energy from $3.7 \pm 0.6 \mu\text{J}/\text{m}^2$ with increasing surface density of oligopeptide. We calculate that a mass density of oligopeptide of less than $1 \text{ ng}/\text{cm}^2$ can lead to a measurable change in the anchoring energy of the nematic liquid crystal. These results suggest that measurements of anchoring energies of liquid crystals on surfaces may offer the basis of quantitative and label-free methods for detecting biomolecules on surfaces.

Introduction

Liquid crystals are materials that spontaneously order over distances that are large (μm) relative to the size of their molecular components (\AA).¹ When placed into contact with nanostructured surfaces, nematic liquid crystals can be anchored in preferred orientations that extend over macroscopic distances from the interface,² thus amplifying the nanoscopic structure of the interface into the visible scale. This paper reports a study that seeks to exploit surface-induced ordering of nematic liquid crystals to report the presence of biomolecules presented at surfaces. The approach is based on measurements of the anchoring energies of liquid crystals at surfaces.

The average orientation assumed by a nematic liquid crystal near a structured surface is referred to as the easy axis (denoted η_0) of the liquid crystal. Many methods can be used to structure surfaces such that they define the easy axis of a liquid crystal, including mechanical shearing of polymer films,^{3–5} controlled illumination of photoactive films,^{6–8} and the oblique deposition of metals and metal oxides.^{2,9} These surfaces orient the liquid crystals through a variety of long-range (e.g., elastic)¹⁰ and short-range (e.g., intermolecular)^{4,5,11} interactions. Recently, we reported investigations of the orientations of liquid crystals at surfaces that present chemical functional groups relevant to the potential use of liquid crystals as amplifier of biomolecular interactions at interfaces.^{12–26} In one approach, self-assembled

monolayers presenting oligomers of ethylene glycol were prepared on surfaces of thin gold films deposited at an oblique (grazing) angle of incidence (Figure 1).^{25,27} In these studies, the structure of the monolayer (e.g., tri(ethylene glycol) versus tetra(ethylene glycol)) was found to influence both the in-plane orientation of η_0 as well as the so-called azimuthal anchoring energy W_{az} . The latter quantity, which quantifies the energy of interaction leading to a particular azimuthal orientation of a liquid crystal, can be defined as

$$\tau = W_{\text{az}} \sin 2\varphi/2 \quad (1)$$

where τ is the magnitude of torque applied to a liquid crystal at a surface (surface-anchoring torque) that leads to a departure of the azimuthal orientation of the director of the liquid crystal from the easy axis by an angle of φ .^{2,27} In this paper, we report that measurements of the anchoring energies of peptide-decorated surfaces are remarkably sensitive to the presence of small quantities of peptide presented at surfaces.

The study reported in this paper builds from recent demonstrations that the spontaneous ordering of liquid crystals can be used to amplify and report a wide range of interfacial phenomena occurring at interfaces, including binding events involving small

* To whom correspondence should be addressed. E-mail: abbot@engr.wisc.edu. Phone: (608) 265-5278. Fax: (608) 262-5434.

(1) de Gennes, P. G. *The Physics of Liquid Crystals*, 1st ed.; Oxford University Press: London, 1974.

(2) Jerome, R. *Rep. Prog. Phys.* **1991**, *54*, 391.

(3) Toney, M. F.; Russell, T. P.; Logan, J. A.; Kikuchi, H.; Sands, J. M.; Kumar, S. K. *Nature* **1995**, *374*, 709.

(4) Stohr, J.; Samant, M. G.; Luning, J.; Callegari, A. C.; Chaudhari, P.; Doyle, J. P.; Lacey, J. A.; Lien, S. A.; Purushothaman, S.; Speidell, J. L. *Science* **2001**, *292*, 2299.

(5) Seo, D.-S.; Muroi, K.; Isogami, T.; Matsuda, H.; Kobayashi, S. *Jpn. J. Appl. Phys.* **1992**, *31*, 2165.

(6) Gibbons, W. M.; Shannon, P. J.; Sun, S.-T.; Swetlin, B. J. *Nature* **1991**, *351*, 49.

(7) Schadt, M.; Seiberle, H.; Schuster, A. *Nature* **1996**, *381*, 212.

(8) Ichimura, K. *Chem. Rev.* **2000**, *100*, 1847.

(9) Janning, J. L. *Appl. Phys. Lett.* **1972**, *21*, 173.

(10) Berreman, D. W. *Phys. Rev. Lett.* **1972**, *28*, 1683.

(11) Feller, M. B.; Chen, W.; Shen, Y. R. *Phys. Rev. A* **1991**, *43*, 6778.

(12) Shah, R. R.; Abbott, N. L. *Langmuir* **2003**, *19*, 275.

(13) Brake, J. M.; Daschner, M. K.; Luk, Y.-Y.; Abbott, N. L. *Science* **2003**, *302*, 2094.

(14) Gupta, V. K.; Skaife, J. J.; Dubrovsky, T. B.; Abbott, N. L. *Science* **1998**, *279*, 2077.

(15) Kim, S.-R.; Abbott, N. L. **2002**, *18*, 5269.

(16) Luk, Y.-Y.; Tingey, M. L.; Hall, D. J.; Israel, B. A.; Murphy, C. J.; Bertics, P. J.; Abbott, N. L. *Langmuir* **2003**, *19*, 1671.

(17) Shah, R. R.; Abbott, N. L. *J. Phys. Chem. B* **2001**, *105*, 4936.

(18) Skaife, J. J.; Abbott, N. L. *Langmuir* **2000**, *16*, 3529.

(19) Skaife, J. J.; Brake, J. M.; Abbott, N. L. *Langmuir* **2001**, *17*, 5448.

(20) Tercero Espinoza, L. A.; Schumann, K. R.; Luk, Y.-Y.; Israel, B. A.; Abbott, N. L. *Langmuir* **2004**, *20*, 2375.

(21) Skaife, J. J.; Abbott, N. L. *Langmuir* **2001**, *17*, 5595.

(22) Shah, R. R.; Abbott, N. L. *J. Am. Chem. Soc.* **1999**, *121*, 11300.

(23) Kim, S.-R.; Teixeira, A. I.; Nealey, P. F.; Wendt, A. E.; Abbott, N. L. *Adv. Mater.* **2002**, *14*, 1468.

(24) Luk, Y.-Y.; Yang, K.-L.; Cadwell, K.; Abbott, N. L. *Surf. Sci.* **2004**, *570*, 43.

(25) Clare, B. H.; Abbott, N. L. *Langmuir* **2005**, *21*, 6451.

(26) Tingey, M. L.; Luk, Y.-Y.; Abbott, N. L. *Adv. Mater.* **2002**, *14*, 1224.

(27) Clare, B. H.; Guzman, O.; de Pablo, J. J.; Abbott, N. L. *Langmuir* **2006**, *22*, 4654.

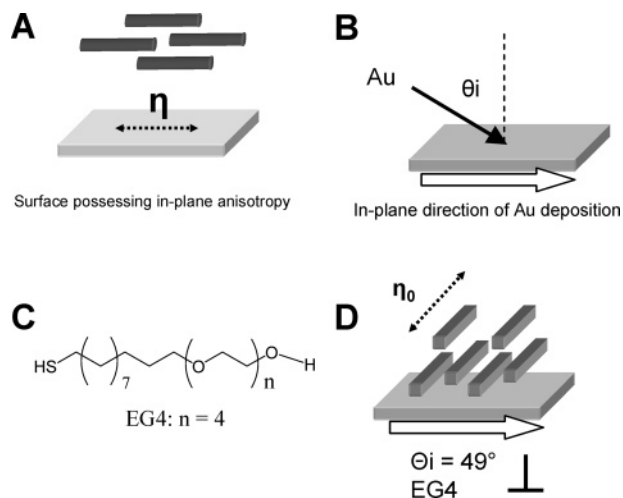


Figure 1. Schematic illustrations of (A) the easy axis of a liquid crystal on a surface, (B) the oblique deposition of gold onto a surface, (C) the molecular structure of the tetra(ethylene glycol)-terminated alkanethiol used in our study, and (D) the orientation of the easy axis of 5CB supported on an obliquely deposited gold film decorated with a monolayer of the compound shown in C.

organic molecules²⁸ and chemical transformations,²² and changes in interfacial structure caused by the binding/immobilization of peptides,²⁵ proteins,^{14,18,19,21} and viruses.²⁰ In these past studies, the presence of increasing amounts of bound peptide or protein was observed to lead to spontaneous changes in the orientations of the liquid crystals as well as the introduction of networks of defects into the liquid crystals. These changes in orientation were reported by the transmission of polarized light through the liquid crystal. The study reported here sought to go beyond these past studies by establishing methods based on liquid crystals that would (1) provide increased sensitivity to the presence of biomolecules on surfaces, (2) provide facile methods to quantify the amount of analyte present at the interface, and (3) provide quantitative information about the strength of interaction of liquid crystals with the biomolecule-decorated interfaces. In particular, we sought to determine if changes in the azimuthal anchoring energy of the nematic liquid crystal 5CB could be measured at surface coverages of biomolecules that are below the thresholds that lead to spontaneous changes in the ordering of the liquid crystals.

The approach reported in this paper to measurement of the azimuthal anchoring energy of peptide-decorated interfaces is a variant of the elastic torque-balance method.^{27,29–31} In brief, when using the torque-balance method, liquid crystals are confined between two surfaces such that η_0 at the top surface is rotated approximately 90° relative to the orientation of η_0 at the bottom surface (Figure 2A). This configuration induces a twist distortion across the film of liquid crystal. For films of liquid crystal that are sufficiently thin, the elastic bulk torque of the liquid crystal competes with the surface-anchoring torque such that the equilibrium position of the director η_d deviates by an angle (φ) from the easy axis of surfaces with finite azimuthal anchoring energies W_{az} . Whereas the conventional torque-balance method uses two identical surfaces, the methodology reported in this paper permits measurement of the anchoring energy on a single, patterned surface. In this modified procedure, the liquid crystal is confined by a second surface (reference plate) that strongly

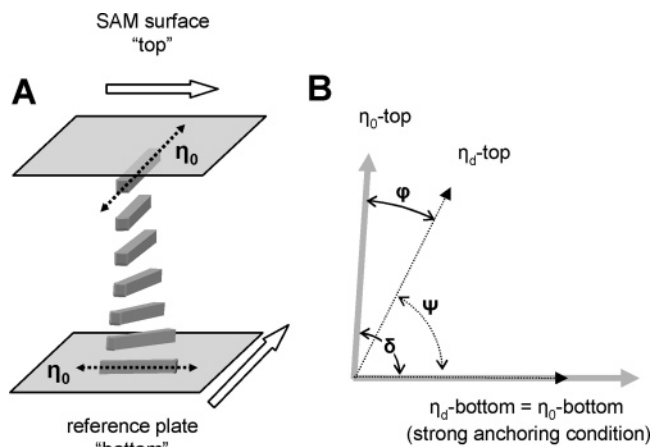


Figure 2. Schematic illustration of (A) twist distortion of liquid crystal between two surfaces with easy axes η_0 and (B) angles that characterize the departure of the director of the liquid crystal from the easy axis at the top surface shown in A.

anchors the liquid crystal, such that deviation of the orientation of the liquid crystal from the easy axis only occurs at the surface of interest, as depicted in Figure 2B. The azimuthal anchoring energy is calculated as

$$W_{az} = \frac{2K_{22}\Psi}{d \sin(2\varphi)} \quad (2)$$

where K_{22} is the twist elastic constant for the liquid crystal, d is the thickness of the film of liquid crystal, and ψ is the twist angle over which the director of the liquid crystal is rotated. The use of surfaces patterned with SAMs and peptides permits simultaneous measurement of multiple values of W_{az} in a single experiment, thus minimizing the volumes of solutions required for surface functionalization and analysis. Specifically, we apply this methodology to determine how the incremental addition of the peptide IYGEFKKKC (a substrate for Src kinase) to an interface leads to changes in azimuthal anchoring energy of a nematic liquid crystal.

Following the description of the Materials and Methods, this paper is organized into two parts. First, we describe experiments that sought to validate the methods reported in this paper for measurement of anchoring energies. These experiments are based on measurements of anchoring energies of nematic 5CB on patterned, ethylene glycol-terminated SAMs. Second, we apply the validated methods to measure the anchoring energies of liquid crystals on surfaces patterned with oligopeptides.

Materials and Methods

Materials. All materials were used as received unless otherwise noted. Fisher's Finest glass slides were obtained from Fisher Scientific (Pittsburgh, PA). Gold (99.999% purity) was obtained from International Advanced Materials (Spring Valley, NY). Titanium (99.99% purity) was obtained from PureTech (Brewster, NY). The nematic liquid crystal 4-cyano-4'-pentyl-biphenyl (5CB) was obtained from EM Industries (New York, NY) sold under the trademark name Licristal (K15). Tetra(ethylene glycol)-terminated alkanethiol (EG4) was synthesized using previously published methods.³² The amine-terminated thiol (EG3-N) was purchased from Prochimia (Poland). The sulfo-succinimidyl 4-(*N*-maleimidomethyl)cyclohexane-1-carboxylate (sulfo-SMCC) linker was obtained from Pierce Biotechnology (Rockford, IL). Ethanol (200-proof) was obtained from Aaper Alcohol (Shelbyville, KY) and purged for at least 1 h with argon

(28) Shah, R. R.; Abbott, N. L. *Science* **2001**, *293*, 1296.

(29) Wood, E. L.; Bradberry, G. W.; Cann, P. S.; Sambles, J. R. *J. Appl. Phys.* **1997**, *82*, 2483.

(30) Polossat, E.; Dozov, I. *Mol. Cryst. Liq. Cryst.* **1996**, *282*, 223.

(31) Fonseca, J. G.; Galerne, Y. *Appl. Phys. Lett.* **2001**, *79*, 2910.

(32) Pale-Grosdemange, C.; Simon, E. S.; Prime, K. L.; Whitesides, G. M. *J. Am. Chem. Soc.* **1991**, *113*, 12.

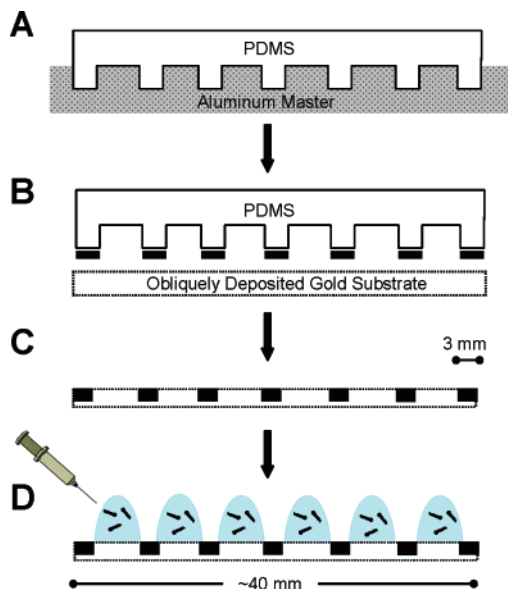


Figure 3. Procedure used to create arrays of SAMs on a single gold film.

gas prior to use. Poly(dimethylsiloxane) (PDMS) elastomeric stamps were prepared using Sylgard 184 silicone elastomer kit obtained from Dow Corning (Midland, MI). Peptides IYGEFKKKC were synthesized at the University of Wisconsin Biotechnology Center and purified by HPLC to yield products with >95% purity. Triethanolamine was obtained in 99% purity from Fisher. Phosphate-buffered saline (PBS) was obtained from Sigma-Aldrich.

Preparation of Gold Films. Glass slides were first cleaned using a piranha solution as outlined in a prior publication.³³ The slides were then positioned within the chamber of an electron beam evaporator such that the angle of incidence of gold onto the substrate (defined with respect to the surface normal) could be manipulated. The incident angles were measured manually using a digital level, with an accuracy of $\pm 2^\circ$. All metal films were deposited at chamber pressures $< 1 \times 10^{-6}$ Torr and at deposition rates of $< 0.2 \text{ \AA/s}$. First, a thin film of titanium (total thickness of 42–60 \AA) was deposited onto the glass substrate to serve as an adhesion layer. Next, semi-transparent films of gold (total thickness 105–140 \AA) were deposited onto the substrate. In the remainder of this paper, these substrates are referred to as “obliquely deposited gold films”. All gold substrates were used within 1 h of removal from the evaporator chamber.

Formation of Patterned Self-assembled Monolayers of Tetra-(ethylene glycol)-Terminated Thiols. The procedure used to create the patterned SAMs is depicted in Figure 3. First, a poly(dimethylsiloxane) (PDMS) elastomeric stamp with raised features (having dimensions of 2–3 mm width and 2–3 mm height) was cast from an aluminum master. The PDMS stamp was inked with a 1 mM ethanolic solution of hexadecanethiol and then gently dried using a stream of nitrogen gas. The stamp was placed in conformal contact with an obliquely deposited gold film for 5–10 s in order to print monolayers of hexadecanethiol onto the surface of the gold film. Next, 1 mM ethanolic solutions of oligo(ethylene glycol)-terminated thiols were prepared using argon-purged ethanol. These solutions were stored under an argon atmosphere to prevent oxidation of the sulfhydryl functionality. Droplets of thiol solutions were applied to the gold substrate, confined between the patterned stripes of hexadecanethiol SAMs (Figure 3D). The substrates were stored in a chamber saturated with ethanol vapor (to prevent droplet evaporation) for 18 h and then rinsed with copious amounts of water and ethanol. The samples were gently dried under a stream of nitrogen gas prior to placing them in contact with 5CB (see below for details).

Preparation of Peptide-Modified SAMs. The chemistry used to attach the oligopeptide IYGEFKKKC to oligo(ethylene glycol)-containing SAMs is described in a previous publication.²⁵ In brief,

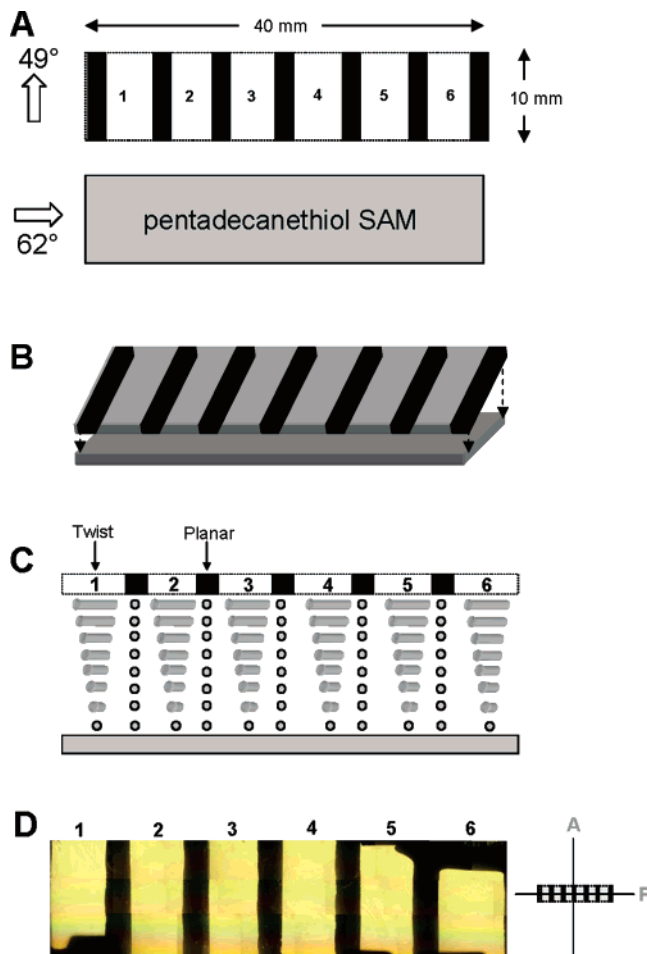


Figure 4. Schematic illustration of (A) surfaces patterned with SAMs, (B) assembly of the surfaces patterned with SAMs into a wedge-shaped cell, and (C) twist distortion of liquid crystal within the cell shown in B. Part (D) is a polarized light micrograph (cross-polars) of 5CB contained in the wedge-shaped cell shown in parts A–C.

patterned SAMs comprised of EG3-N and EG4 were prepared by the above method, using 1 mM ethanolic solutions of thiols (mole fraction of EG3-N ($\chi_{\text{EG3-N}}$) systematically varied from 0 to 0.05). After formation of the SAM for 18 h, surfaces were rinsed with copious amounts of ethanol and water and gently dried under a stream of nitrogen gas. Next, 2 mM solutions of the linker sulfo-SMCC (0.1 M triethanolamine buffer, pH 7.0) were applied as droplets to the monolayers for 30 min. These surfaces were rinsed briefly in water and dried. Next, 250 μM solutions of the cysteine-terminated peptide (also in 0.1 M triethanolamine buffer, pH 7.0) were applied as droplets to the surface. The substrates were stored in a chamber saturated with water vapor (to prevent droplet evaporation) for 3 h. These surfaces were rinsed three times with 5 mL of 0.1 M triethanolamine buffer and once with water and then dried prior to use.

Ellipsometry. The formation of SAMs was confirmed using a Rudolph-EL II ellipsometer (633 nm light at 70° grazing angle of incidence) and reflective gold substrates (2000 \AA gold/100 \AA titanium adhesion layer, both deposited at normal incidence). Three to five measurements were recorded for each sample. To estimate the thickness of the SAM, we used a 2-slab model assuming that the organic film supported on the gold has a refractive index of 1.45. The ellipsometric thicknesses of the SAMs were confirmed to correspond to those values reported previously by us.^{25, 27}

Preparation of Optical Cells Containing Liquid Crystal. First, a reference plate was prepared by immersing an obliquely deposited gold substrate (angle of incidence $\theta_i = 62^\circ$) into a 1 mM ethanolic solution of pentadecanethiol for 2 h. The sample was rinsed with

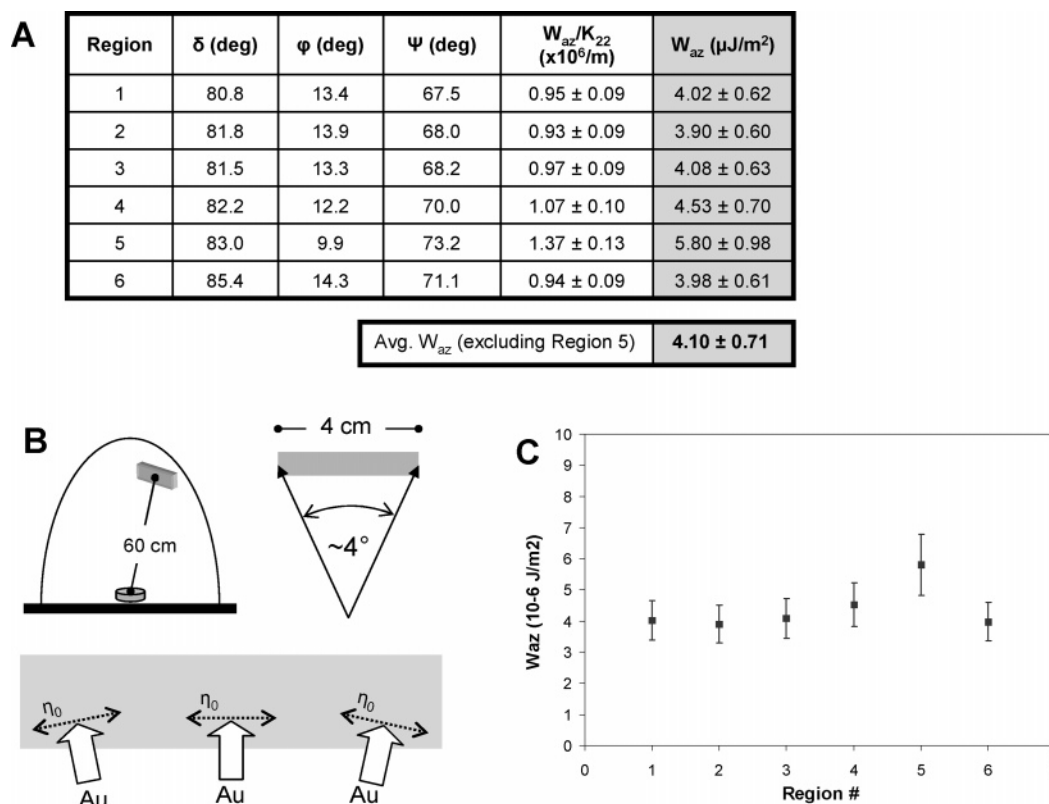


Figure 5. Results of anchoring energy measurements of 5CB on patterned EG4-terminated SAMs. (A) Tabulated data characterizing the orientation of the liquid crystal on the patterned surface. See text for details. (B) Schematic illustration of the deposition of gold onto a planar substrate (length 4 cm) in an electron beam evaporator. (C) Measured values of the anchoring energy on EG4-terminated SAMs. See text for discussion of anchoring energy measured on Region 5.

copious amounts of ethanol and dried under a stream of nitrogen gas. A patterned SAM, prepared as described above, was paired with the reference plate such that the in-plane direction of gold deposition of the reference plate was rotated approximately 90° relative to the in-plane direction of gold deposition of the patterned surface (see Figure 4A). The surfaces were separated by a $12 \mu\text{m}$ spacer (Mylar film) at one end, and were not separated by a spacer at the other end, to create a wedge-shaped cell (see Figure 4B). The surfaces were held together using “bulldog” clips. The optical cell and 5CB were both warmed to approximately $40\text{--}45^\circ\text{C}$ (above the clearing point for 5CB). 5CB was then drawn into the optical cell by capillary action and slowly cooled to room temperature (22°C). As a precaution, measurements of the optical properties of the liquid crystal were taken 30 min after cooling to room temperature, as both temperature³⁴ and age of the sample (surface gliding)³¹ have been reported in some instances to influence the anchoring strength of liquid crystals.

Optical Determination of d , δ , Ψ , and φ . The optical methods used to determine the thicknesses of the films of liquid crystal (d), the angles formed between the easy axes of each confining substrate (δ), the angle over which the liquid crystal forms a twist (ψ), and the angle of deviation of the director from the easy axis (φ) are described in detail in a previous publication²⁷ and are adapted from methods described by Fonseca and Galerne.³¹ Measurements were recorded using a polarized light microscope (BX 60, Olympus) equipped with an X–Y translating stage and fitted with a digital camera for image capture.

Results and Discussion

Validation of Methodology for Measurement of the Anchoring Energy. We have previously reported use of the torque-balance method to determine the anchoring energy of

nematic 5CB on SAMs by using optical cells prepared from two identical surfaces.²⁷ The methodology for measuring the anchoring energy that is reported in this paper differs from our past work because we sought to make use of a reference plate and a patterned SAM to simultaneously measure multiple anchoring energies on the patterned surface. Our implementation of the approach based on use of a reference plate is simplified by use of a surface that anchors the liquid crystal sufficiently strongly that the deviation of the director from the easy axis of the reference plate is negligible. The first experiments we performed sought to validate our methodology for measuring anchoring energies based on use of a reference surface that provides strong anchoring. Validation was based on measurement of W_{az} of tetra(ethylene glycol)-terminated SAMs, the values of which we have previously reported.²⁷

For these first experiments, we prepared surfaces patterned with regions of tetra(ethylene glycol)-terminated SAMs, as described in the Methods section and depicted in Figure 4A. The patterned SAMs were prepared on gold films deposited at an angle of incidence of 49° from the surface normal. As a reference plate, we used a SAM formed from pentadecanethiol supported on an obliquely deposited gold film deposited at an angle of incidence of $\theta_i = 62^\circ$. The results of our past studies^{19,27} demonstrate that such a high angle of deposition of the gold will lead to a reference plate with strong anchoring properties. We prepared a wedge-shaped optical cell using the patterned surface and the above-described reference surface (see Methods and Figure 4B) and filled the cell with 5CB.

Figure 4D shows the optical appearance of the liquid crystal cell when viewed between crossed polars (transmission mode). The bright regions (labeled 1–6 in Figure 4D) correspond to regions of the patterned surface decorated with the tetra(ethylene

(34) Imura, Y.; Kobayashi, N.; Kobayashi, S. *Jpn. J. Appl. Phys.* **1995**, *34*, 1935.

glycol)-terminated SAMs. These regions appear bright because plane-polarized light emanating from the source (P) is rotated as it passes through a twisted liquid crystal (see Figure 4C) and is therefore transmitted through the analyzer (A). The dark bands in Figure 4D correspond to regions of the patterned surface decorated with SAMs printed from hexadecanethiol. In these regions, the liquid crystal is not twisted (see Figure 4C), the polarization of light transmitted through the sample is not rotated, and thus light is extinguished by the analyzer.³⁵

Using optical methods reported previously (based on rotation of the sample between the polarizers) and the sample shown in Figure 4D,²⁷ we next measured the relative orientation of the *easy axes* of the two confining surfaces (see Figure 2B, angle δ) in each of the six regions shown in Figure 4D to determine the uniformity of the obliquely deposited gold films used in these experiments. Our findings are summarized in the second column of the table shown in Figure 5A. These measurements reveal that there is a systematic variation in δ from the leftmost region of the substrate (Region 1) to the rightmost region of the substrate (Region 6), from 80.8° to 85.4° , respectively. The observed variation in δ reflects small changes in the orientation of the easy axis (η_0) at the top (patterned) substrate, as depicted in the angle diagram in Figure 2B. The orientation of η_0 at the top surface is dependent on the in-plane direction of the deposition of gold used to create the top surface. We thought it likely that we would find evidence of small variations in the direction of gold deposition (as suggested by the above-described measurements) due to the geometry of the electron beam evaporator used to prepare the gold films (Figure 5B). During deposition of the gold films, the substrate is held at a distance of approximately 600 mm from the gold source. Each sample used in this study has a width of 40 mm. Based on this geometry, we calculate the difference in the in-plane angle of gold deposition, from the leftmost edge to the rightmost edge of the substrate, to be approximately 4° . This estimation is in agreement with the variations in δ that we report above. Here we make two comments on these measurements. First, we note that a reduction in sample size, or an increase in the distance between the source and substrate during deposition, will lead to smaller variations in δ within a single sample. Second, we emphasize that the above variation in the orientation of the easy axis does not prevent accurate determination of the anchoring energy of the liquid crystal. The anchoring energy is an intrinsic property of the interface and the methodology used below incorporates the measured variation of δ into the calculated values of the anchoring energy.

We next determined the equilibrium orientation of the director (η_d , expressed as angles ψ and φ , see angle diagram in Figure 2B) in each of the bright regions shown in Figure 4D. The orientation of the director was determined in each region at a fixed thickness $d = 5.5 \pm 0.5 \mu\text{m}$. Using the torque-balance expression (see eq 2) and the measurements for δ , φ , and ψ summarized in Figure 5A, we determined W_{az} in each of the six tetra(ethylene glycol) regions shown in Figure 4D.³⁶ The values of W_{az} also appear in Figure 5A and are graphically represented in Figure 5C. Error bars in the vertical direction reflect the uncertainties in our determination of angles ψ and φ and thickness d .

Inspection of Figure 5C reveals good agreement between the values of W_{az} with the exception of W_{az} determined for Region 5. As described above, each of the regions of the tetra(ethylene glycol)-terminated SAMs were prepared by placement of a droplet of an ethanolic solution on the substrate for 18 h. Unlike Regions

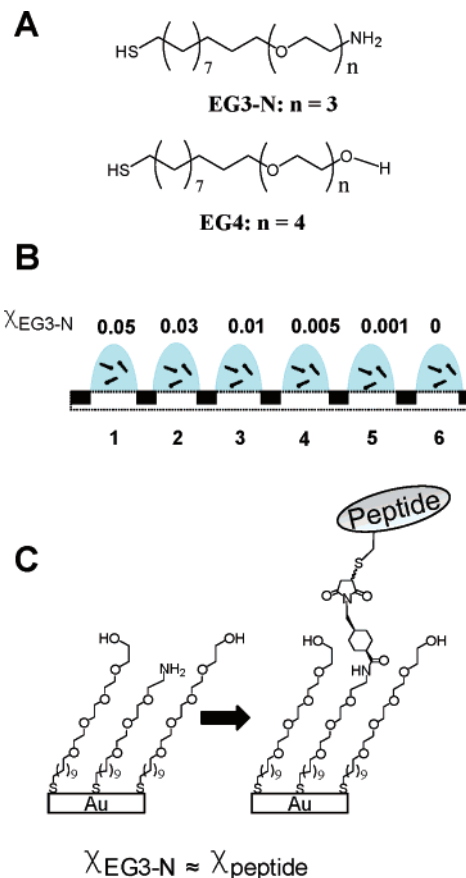


Figure 6. Schematic illustrations of (A) compounds used to form mixed SAMs on which the peptides were immobilized, (B) procedure used to form arrays of patterned SAMs, with each pixel of an array containing a different density of peptide, and (C) mixed SAMs to which peptides were immobilized.

1–4 and 6, we observed the droplet confined to Region 5 to evaporate during the 18 h of incubation (even when precautions were taken to minimize evaporation, i.e., storing the substrate in a chamber saturated with ethanol vapor). We speculate that the anomalous value of the anchoring energy measured on Region 5 reflects differences in the structure of the interface caused by evaporation (e.g., incomplete monolayer formation, physisorption, or formation of multilayers). In support of this proposition, in a study to be reported elsewhere, we have determined that the anchoring energies of liquid crystals measured on SAMs do depend on factors such as time of formation of the SAMs.

Finally, we compare the values of the anchoring energies reported in Figure 5 to values reported in a previous publication (using a methodology that involved two tetra(ethylene glycol)-terminated SAMs, not the reference surface).²⁷ In our previous study, we determined W_{az} for 5CB in contact with tetra(ethylene glycol)-terminated SAMs to be 1.4 ± 0.3 and $5.5 \pm 0.7 \mu\text{J}/\text{m}^2$ when using gold films deposited at $\theta_i = 41^\circ$ and $\theta_i = 58^\circ$, respectively.²⁷ The average that we report in this paper, namely, $4.1 \pm 0.7 \mu\text{J}/\text{m}^2$ (based on Regions 1–4 and 6, as discussed above), when using gold films prepared at intermediate deposition angles of $\theta_i = 49^\circ$ falls between these two values. These results, when combined, support our conclusion that a methodology based on patterned SAMs and a strong-anchoring reference plate can be used to provide consistent measurements of anchoring energies. Below we use this methodology to determine the influence of peptides immobilized on surfaces on the anchoring energy of 5CB.

Anchoring Energy of Liquid Crystal in Contact with Peptide-Modified Surfaces. Peptide-modified SAMs, prepared

(35) Hartshorne, N. H.; Stuart, A. *Crystals and the Polarizing Microscope*, 4th ed.; Edward Arnold Publishers, Ltd.: London, 1970.

(36) Toyooka, T.; Chen, G.-P.; Takezoe, H.; Fukuda, A. *Jpn. J. Appl. Phys.* **1987**, *26*, 1959.

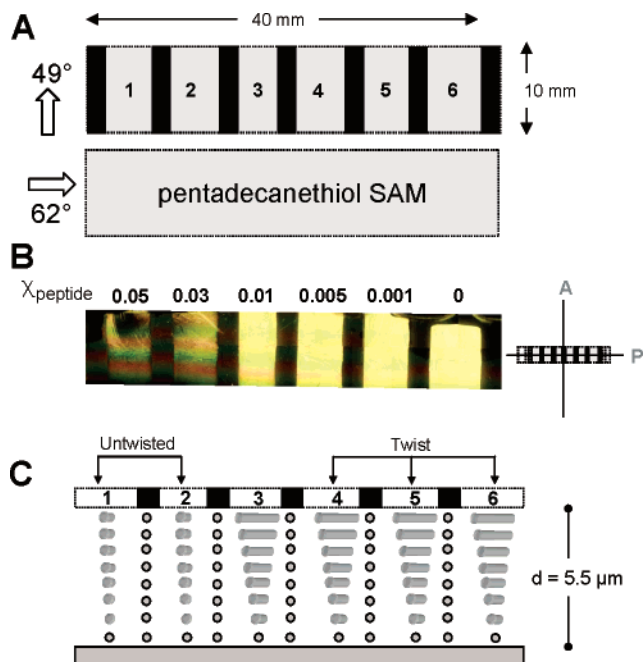


Figure 7. (A) Schematic illustration of surfaces patterned with SAMs. (B) Polarized light micrograph (cross-polars) of 5CB in contact with peptide-decorated SAMs. (C) Schematic illustration of twist distortion of liquid crystal within the cell shown in B.

using previously published synthetic procedures,²⁵ were arrayed onto an obliquely deposited gold substrate ($\theta_i = 49^\circ$). Briefly, we formed two-component SAMs (see Figure 6A) by applying to the gold substrate a series of thiol solutions comprised of an amine-terminated tri(ethyleneglycol) alkanethiol (EG3-N) and a tetra(ethylene glycol)-terminated alkanethiol (EG4), where the mole fraction of the amine component EG3-N was systematically

increased ($\chi_{\text{EG3-N}} = 0$ to 0.05), as shown in Figure 6B. Next, using procedures described in the Methods section, we covalently attached the terminal cysteine residue of the peptide IYGEFKKKC³⁷⁻³⁹ to the amine groups presented by the monolayer (Figure 6C). Using this procedure, we created patterned SAMs with various densities of peptide molecules grafted onto the SAMs.

Similar to the study reported above, we next assembled an optical cell comprised of the peptide-modified array and a reference plate, as shown in Figure 7A. The optical appearance of this sample, when viewed using polarized light microscopy (crossed polars), is shown in Figure 7B. Visual inspection of Figure 7B reveals that the brightness of the liquid crystal varies with the amount of peptide immobilized on the SAM. When in contact with the EG4 SAM ($\chi_{\text{peptide}} = 0$), the 5CB appears bright when viewed between the crossed polars. This bright appearance indicates a twist distortion of the liquid crystal, similar to that seen in the images in Figure 4D. Moving from right to left across Figure 7B, liquid crystal in contact with surfaces that present densities of immobilized peptides with $\chi_{\text{peptide}} = 0.001$, 0.005, and 0.01 also appears bright, indicative of some level of twist within the liquid crystal. In contrast, when in contact with SAMs that present higher densities of immobilized peptides ($\chi_{\text{peptide}} = 0.03$, 0.05), the liquid crystal appears significantly less bright to the naked eye. The dark optical appearance indicates that the liquid crystal is less twisted in these regions. Figure 7C provides a qualitative depiction of the orientations of the LCs in Figure 7B, as a function of increasing density of immobilized peptide.

Figure 8A reports a summary of our measurements of δ , ψ , and φ that quantify the orientations of the liquid crystal discussed above. From Figure 8A, we make several observations. First, similar to Figure 5A, we note a variation in δ of approximately 4° across the sample. Second, we note that the angle at which the director deviates from the easy axis (φ) is a function of the

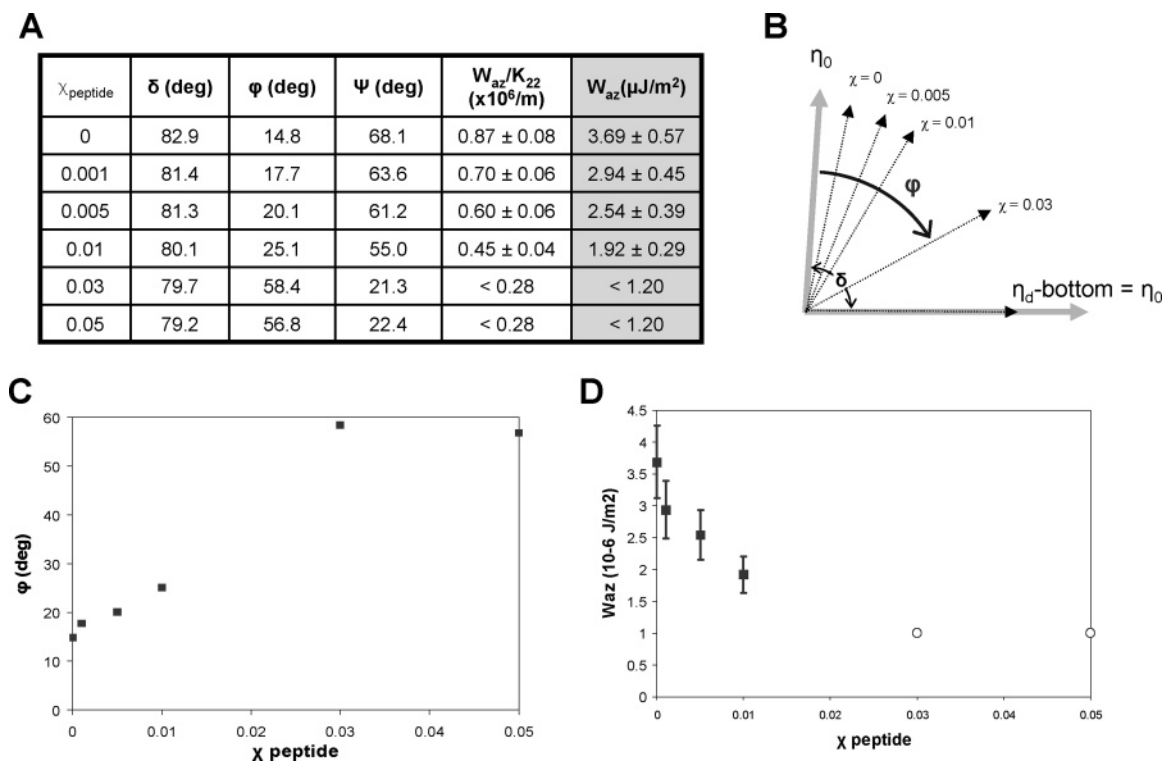


Figure 8. Results of anchoring energy measurements of 5CB on peptide-decorated surfaces. (A) Tabulated data characterizing the orientation of the liquid crystal on the peptide-decorated surfaces. See text for details. (B) Schematic illustration of the departure of the director from the easy axis on the peptide-decorated surfaces. (C) Measured values of the deviation of the director from the easy axis on peptide-decorated surfaces. (D) The anchoring energy of 5CB on peptide-decorated surfaces.

density of peptide in the SAM. Between $\chi_{\text{peptide}} = 0$ and $\chi_{\text{peptide}} = 0.01$, the angle φ increases from 14.8° to 25.1° . A further increase in the density of peptide to $\chi_{\text{peptide}} = 0.03$ leads to a substantial increase in φ to 58.4° . The value of φ does not appear to increase further at higher peptide coverages ($\chi_{\text{peptide}} = 0.05$, $\varphi = 56.8^\circ$). The influence of increasing χ_{peptide} on the equilibrium position of the director (and the angle φ) is summarized pictorially in Figure 8B and graphically in Figure 8C.

Next, we calculated W_{az} using the measurements summarized in Figure 8A and the torque-balance model given in eq 2. This model uses an approximation for surface-anchoring torque proposed by Rapini and Papoular⁴⁰ that is not valid for $\varphi > 45^\circ$.²⁹ The measured values of φ for liquid crystal in contact with $\chi_{\text{peptide}} = 0.05$ and $\chi_{\text{peptide}} = 0.03$ exceeded this limitation (when recorded at a film thickness of liquid crystal of $5.5 \pm 0.5 \mu\text{m}$, as determined by observation of interference colors using a polarized light microscope²⁷). The large value of φ measured on surfaces with $\chi_{\text{peptide}} = 0.05$ and $\chi_{\text{peptide}} = 0.03$ suggests very weak anchoring at those interfaces. For the reasons stated above, we can only place an upper bound on the anchoring energy on these surfaces ($< 1.20 \mu\text{J}/\text{m}^2$). We note here that in future studies we aim to extend the range of W_{az} that can be experimentally accessed by (1) using liquid crystal films of greater thickness or (2) using liquid crystals that have different elastic constants K_{22} .

For the surfaces with the low densities of peptides, we used eq 2 to calculate W_{az} (Figures 8A and 8D). We note here that the uncertainties reported in our measurement of W_{az} reflect the uncertainty in our experimental determination of thickness (d) and the angle quantities (φ and ψ), as well as uncertainties in the experimental determination of K_{22} .^{36,32} From our measurements of W_{az} in Figure 8D, we make three observations. First, the measurement of W_{az} for $\chi_{\text{peptide}} = 0$ ($3.7 \pm 0.6 \mu\text{J}/\text{m}^2$) agrees well with our measurements reported in Figure 5 ($4.1 \pm 0.7 \mu\text{J}/\text{m}^2$). Second, we conclude that there is a systematic decrease in the measured value of W_{az} with increasing density of peptide immobilized on the surface. The value of W_{az} decreases from 3.7 ± 0.6 to $1.9 \pm 0.3 \mu\text{J}/\text{m}^2$ as the density of peptide on the surface increases from $\chi_{\text{peptide}} = 0$ to $\chi_{\text{peptide}} = 0.01$. Our measurements of anchoring energies for surfaces that present low densities of immobilized peptides are interesting in light of our past observations regarding the use of liquid crystals to detect the presence of peptides and proteins at surfaces: the orientations of liquid crystals were observed to become nonuniform on surfaces that presented a threshold amount of bound peptide or protein.^{14,18,19,21} In contrast, the measurements reported in Figures 7 and 8 of this paper show that low densities of immobilized peptides can lead to uniform orientations of liquid crystals but with values of anchoring energies that change systematically with incremental addition of peptide to the interface. From these combined results, we draw an important conclusion: that in the case of peptides immobilized onto SAMs, a measurable and systematic reduction in W_{az} precedes a spontaneous change in orientation of the liquid crystal (that is, a change in the orientation of the easy axis). The measurement of W_{az} provides, therefore, a means to increase the sensitivity of methods based on liquid crystals for amplifying and detecting biomolecules at interfaces.

Inspection of Figure 8D reveals that the experiments reported in this paper permit a density of peptides corresponding to χ_{peptide}

$= 0.005$ to be distinguished from $\chi_{\text{peptide}} = 0$. We have estimated the mass density of peptide on the surface corresponding to $\chi_{\text{peptide}} = 0.005$ by assuming that (i) the mole fraction of amine-terminated tri(ethylene glycol) terminated alkanethiol in the mixed monolayer is the same as the solution composition and (iii) that all amine-terminated thiols within the mixed monolayer react to immobilize one peptide molecule (molecular weight 1115.5 g/mol), which will likely lead to an overestimation of the amount of peptide on the surface. Using these assumptions, we calculate that the anchoring energy of the liquid crystal is measurably changed by the presence of $1 \text{ ng}/\text{cm}^2$ of peptide on the surface. We note that this estimate is supported by results of a previous study in which the immobilization of the same peptide on a surface with $\chi_{\text{peptide}} = 0.01$ leads to an ellipsometric thickness of peptide that was below the measurable level ($< 0.1 \text{ nm}$).²⁵ This amount of peptide is comparable to the sensitivity that has been reported for other label-free methodologies used to measure biomolecular binding events and/or surface adsorption phenomena, including surface plasmon resonance spectroscopy (SPR, $\sim 2 \text{ ng}/\text{cm}^2$),⁴¹ optical waveguide lightmode spectroscopy (OWLS, $\sim 1 \text{ ng}/\text{cm}^2$),⁴² and attenuated total reflection infrared absorption spectroscopy (ATR-IR, $\sim 1 \text{ ng}/\text{cm}^2$).⁴³ In future publications, we will report the results of ongoing studies that seek to increase further the precision and sensitivity of methods for detection of biomolecules on surfaces using measurement of the anchoring energies of liquid crystals. These studies will also investigate ways of manipulating the dynamic range of measurements of anchoring energies and present a more complete comparison to the above-described analytical methods.

Conclusions

The principal conclusions of the work reported in this paper are 3-fold. First, we have established a methodology that permits measurement of the anchoring energies of liquid crystals on surfaces patterned with areas with differing densities of peptides. Such a methodology is readily applicable to measurements of anchoring energies of liquid crystals on libraries of molecules arrayed on surfaces. Second, our measurements reveal that there are systematic decreases in the anchoring energies of the nematic liquid crystal 5CB on surfaces with increasing densities of the peptide IYGEFKKKC. Mass densities of peptides as low as $1 \text{ ng}/\text{cm}^2$ (or 1 peptide molecule per 50 nm^2) lead to changes in the anchoring energy. Third, and perhaps most importantly, we observed measurable changes in the anchoring energy to precede changes in the easy axis of a liquid crystal, suggesting that measurements of anchoring energy may provide a sensitive and quantifiable means of using liquid crystals to amplify molecular and biomolecular interactions at interfaces. The results described in this paper provide a foundation for future studies that will seek to use measurements of anchoring energies to study the interfacial activities of proteins, including enzymes.

Acknowledgment. This research was partially supported by the National Science Foundation (DMR 0079983, BES 0330333, CTS-040815) and the National Institutes of Health (R01 CA108467-01). The authors thank Professors Bob Hamers and Paul Bertics of the University of Wisconsin-Madison for insightful comments.

LA0604578

(37) Houseman, B. T.; Huh, J. H.; Kron, S. J.; Mrksich, M. *Nature Biotechnology* **2002**, *20*, 270.

(38) Luttrell, D. K.; Lee, A.; Lansing, T. J.; Crosby, R. M.; Jung, K. D.; Willard, D.; Luther, M.; Rodriguez, M.; Berman, J.; Gilmer, T. M. *PNAS* **1994**, *91*, 83.

(39) Martin, G. S. *Nature Rev. Mol. Cell. Biol.* **2001**, *2*, 467.

(40) Rapini, A.; Papoular, M. *J. Phys. Colloq. (France)* **1969**, *4*, 54.

(41) Whalen, R. J.; Wohland, T.; Neumann, L.; Huang, B.; Kobilka, B. K.; Zare, R. N. *Anal. Chem.* **2002**, *74*, 4570.

(42) Bearinger, J. P.; Voros, J.; Hubbell, J. A.; Textor, M. *Biotechnol. Bioeng.* **2003**, *82*, 465.

(43) Rigler, P.; Ulrich, W.-P.; Hoffman, P.; Mayer, M.; Vogel, H. *ChemPhysChem* **2003**, *4*, 268.